*Defect and Diffusion Forum* *Online: 2019-01-22*
*ISSN: 1662-9507, Vol. 390, pp 32-40*
*doi:10.4028/www.scientific.net/DDF.390.32*


# Heat Treatments Effects on Nickel-Based Superalloy Inconel 713C

Breno Boretti Galizoni[1,*], Antônio Augusto Couto[2], Danieli Aparecida Pereira Reis[1, 3]

[1]Instituto Tecnológico de Aeronáutica, São José dos Campos, CEP 12228-900, Brazil.

[2]Instituto de Pesquisas Energéticas e Nucleares and Mackenzie, São Paulo, CEP 05508-900, Brazil.

[3]Universidade Federal de São Paulo, São José dos Campos, CEP 12231-280, Brazil.

[1*]breno.galizoni@gmail.com, [2]danielireis@gmail.com, [3]acouto@ipen.br

**Keywords:** Heat Treatment, Superalloy, Inconel 713C

**Abstract.** The purpose of this work is to study the effect of heat treatments on the microstructure of the nickel-based superalloy Inconel 713C. Three different conditions were studied and the results compared: (1) as cast; (2) solution treatment (1,179°C/2h) and (3) stabilizing treatment (1,179°C/2h plus 926°C/16h). Inconel 713C is normally used in the as-cast condition, an improvement in the 980°C stress-rupture life is often obtained by a solution heat treatment. However, the material in this condition tested under high stress at 730°C shows a marked decreased in rupture life and ductility [1]. The mechanical resistance in creep increases in Inconel 713C by precipitation hardening phase, such γ' ($Ni_3Al$) formed during the heat treatments [2]. The characterization techniques used was: chemical analysis, hardness test, X-ray diffraction, optical microscope and scanning electron microscopy (SEM), EDS analyzes and thermocalculation. The heat treatments modified the dendritic structure, reducing the acicularity. The SEM and EDS analysis illustrated the γ, γ' and carbides. The matrix phase (γ), has in its constitution the precipitation of the γ' phase, in a cubic form, and in some regions, veins of carbides were modified with the heat treatments.

## Intoduction

The severe crisis that hit the economy and, consequently, the aeronautics market in the early 21st century, led aircraft and engine manufacturers to develop more efficient products. New generations of aircraft had aerodynamically improved wings, increased use of composite materials and new aluminum alloy, as well as new manufacturing processes which contributed to weight reduction [1].

Aircraft engine provides some of the most demanding applications for structural materials. Moderns turbine engines operate at high temperatures and stresses, and engine components are often subject to damaging corrosion, oxidation, and erosion conditions. These engines convert fuel energy into propulsive thrust. During the past several decades, higher engine performance has been achieved by increasing turbine gas temperature and by increasing the efficiency of each engine stage [2-11].

Since the development of gas turbine engines for defense jet aircraft, the application of materials in high temperature has been studied. The term superalloy was first used in the mid-1940s to describe high-temperature alloys that could not only be used at elevated temperature but maintained their strength and toughness at elevated temperature. The term referred to nickel- and cobalt-alloys [12].

Superalloys are largely employed in the manufacture of gas turbine components, such as blades, rotors, and vanes. These applications are the result of early developments, originally carried out for military and civilian aviation, which were transferred to the power generation industry. Two techniques were extremely relevant to the production and development of parts manufactured in superalloys: vacuum furnace's technology and investment casting. Additionally, the complex geometry of gas turbine components, such as blades, and rotors, does not allow the intense use of

machining processes. In this sense, the use of investment casting techniques was decisive for the success of superalloy's products with the use of Inconel 713C [13-25].

The objective of this work is to evaluate the effect of heat treatment in the microstructure of Inconel 713C, through chemical analysis, hardness test, X-ray diffraction, optical microscope and scanning electron microscopy (SEM), EDS analyzes and thermocalculation.

## Material and Methods

### *Material*

The material used was the nickel-based superalloy Inconel 713C supplied by Açotécnica S.A. as a conventionally casted rod. The chemical composition is (in wt.%) 73.0Ni – 0.14C – 13.0Cr – 4.8Mo – 2.3Cb (Nb) – 0.75Ti – 6.0Al – 0.010B – 0.10Zr in % weight. [17]. The casting of the alloy is a procedure in vacuum melt furnace. The minimum tensile strength and yield strength at 0.2% offset are 758 MPa and 689 MPa respectively [17].

### *Heat Treatment*

Two heat treatments were realized, one solubilization treatment performed by heating with 10°C per minute rate until 1,176°C for 2 hours. The second treatment, aging, was realized in samples that were already solubilized and it consists in heating with 10°C per minute rate until 927°C for 16 hours. The heat treatment routes are shown in Fig. 1.

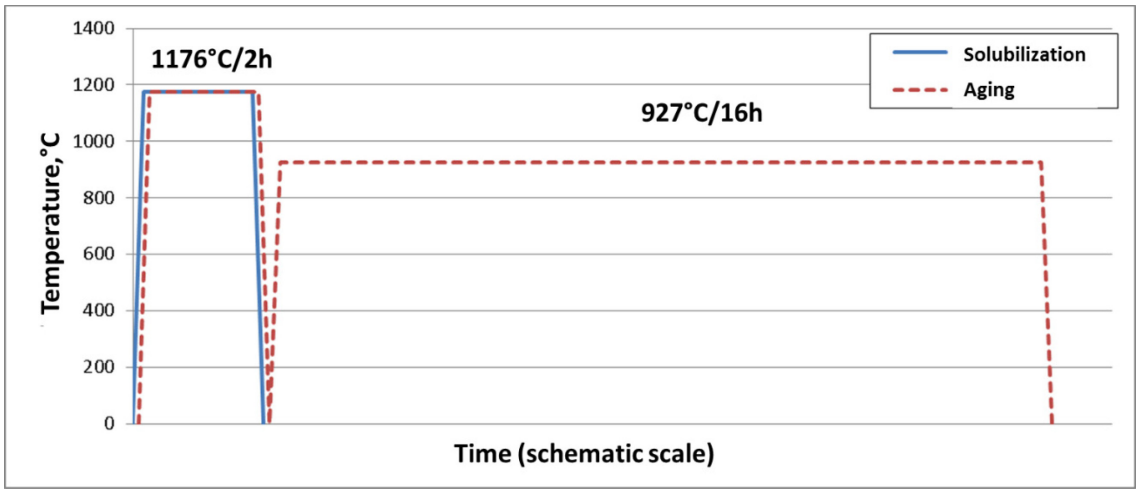


Figure 1. Heat treatments curve realized in the Inconel 713C samples.

The heat treatments were performed in a tubular furnace Lindberg/Blue M (100V/50A/50kW). After the heat treatments, three conditions of Inconel 713C were obtained: as cast, solubilized and aged.

### *Chemical analysis*

The received materials were tested and the samples heat treated, and the results were compared with the international specification of the alloy, AMS 5391 [17]. The analyses of optical emission spectroscopy were carried out in Spectromaxx equipment.

### *Hardness test*

Rockwell C hardness measurements (HRC), with a 15N test load, were performed using Tech LC 200RB equipment. The measurements were obtained on the three samples conditions, as-cast, solubilized and aged.

### *X-ray diffraction*

The X-ray diffraction experiments at room temperature were performed in Panalytical Empyrean equipment using Ni-filtered Cu-Kα radiation, angular interval (2θ) from 10 to 120°, angular step of 0.02°, and counting time of 30 sec.

***Microstructural analysis***

The analyses of the Inconel 713C microstructure after the heat treatments were carried out in the cross sections of the specimens by optical microscopy. The samples were cut, mechanically polished and electrochemically etched – 3% sulfuric acid at 3 volts for 5-10 seconds. A Zeiss Axio Imager Scope A1 microscope was used for microstructure visualization. The scanning electron microscope (SEM) used was a Tescan Vega 3 XMU with Energy-dispersive X-ray spectroscopy (EDS) coupled.

***Thermocalculation***

The phase stability evaluation was carried out using Thermo-Calc Software and TTN18/Ni-based superalloys, database version 8 [18]. The purposes of the calculation were predicting the phase transformation temperatures, the elemental composition of the microstructures in off-equilibrium conditions (ScheilModel).

## Results and Discussion

***Chemical analysis results***

The characterizations by chemical analysis of the main elements, the percentage by weight, were performed in three samples, each with a different heat treatment – as cast, solubilized and aged. The results obtained (in wt.%), as well as the comparison with the international standard AMS 5391 [17], are indicated in Table 1.

Table 1. Results of the chemical analyze of the Inconel 713C samples compared to the international standard AMS 5391.

| **Chemical analysis of Inconel 713C** | | | | |
|---|---|---|---|---|
| **Elements (wt.%)** | **AMS 5391** | **As cast** | **Solubilized** | **Aged** |
| **Cr** | 12.00 – 14.00 | 13.32 | 13.58 | 13.70 |
| **Mo** | 2.80 – 5.20 | 3.85 | 3.93 | 3.96 |
| **Al** | 5.50 – 6.50 | 5.62 | 5.72 | 5.60 |
| **Ti** | 0.50 – 1.00 | 0.67 | 0.70 | 0.67 |
| **C** | 0.08 – 0.20 | 0.11 | 0.11 | 0.11 |
| **B** | 0.005 – 0.015 | 0.009 | 0.01 | 0.009 |
| **Zr** | 0.05 – 0.15 | 0.076 | 0.085 | 0.083 |
| **Si** | max. 0.50 | 0.15 | 0.15 | 0.13 |
| **Mn** | max. 0.25 | 0.012 | 0.012 | 0.007 |
| **Fe** | max. 2.50 | 0.89 | 0.86 | 0.89 |
| **Cu** | max. 0.50 | 0.004 | 0.005 | 0.004 |
| **Ni** | balance | balance | balance | balance |

The comparison of the results obtained in the chemical analyzes with the AMS 5391 standard met the requirements described in the standard. The chemical analysis of the material in the as-cast condition considered to be satisfactory is essential to evaluate the quality of the material manufactured by Açotecnica S.A. and to enable the continuity of the work. The results of the analysis of the other two heat treatments, solubilization, and aging, are important to prove the non-variation of the chemical composition throughout the treatments.

The formation of matrix phase γ (CFC - austenitic) occurs by the presence of chemical elements nickel, chromium, and molybdenum. On the other hand, the presence of the aluminum and titanium elements are responsible for the formation of intermetallic hardening phases of type $A_3B$ - $Ni_3$(Al, Ti), the best known being the γ' phase. The precipitation of the γ' phase in the matrix phase γ contributes to the increase of the mechanical resistance; this is due to the resistance of the precipitates to the movement of the dislocations present in the material.

***Hardness measurements***

Table 2 shows the average hardness data of five samples in each of the three heat treatment conditions (as cast, solubilized and aged).

Table 2. Results of the Rockwell C hardness tests in the samples.

| Inconel 713C | Hardness (HRC) |
|---|---|
| **As cast** | 36 ± 1 |
| **Solubilized** | 40 ± 1 |
| **Aged** | 37 ± 1 |

The alloy Inconel 713C is a casted alloy, and does not have a hardness specified in international standard (AMS 5391), however a hardness range of 30 - 42 HRC (Rockwell C) is defined [17]. All results obtained in the hardness tests in the three heat treatment conditions were within this range.

For the samples heat-treated, a variation in the hardness was evidenced. The solubilized samples showed an increase of less than 10% in the hardness values obtained. On the other hand, the aged samples showed a decrease in the hardness in comparison with the solubilized, returning to the level of hardness of the as casted samples.

***X-ray diffraction results***

The X-ray diffraction analysis was performed in the three heat treatment conditions, and we showed in all conditions peaks at the same crystallographic angles, but with different intensities.

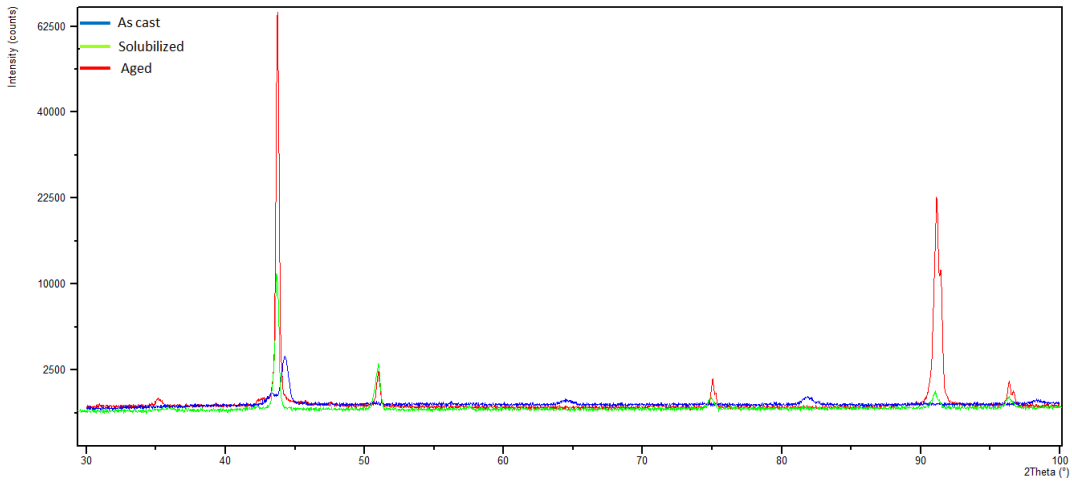


Figure 2. X-ray diffraction images of the samples (as cast, solubilized and aged).

***Microstructural analysis***

The typical microstructure of Inconel cast products is a γ-phase matrix whose dendritic structure is highly influenced by the casting process, such as cooling and solidification rate.

The presence of defects such as porosity, segregation, and inclusions of non-metallic is normal in materials in the as-cast state, without thermomechanical treatments. In optical microscopy analysis, it is possible to observe the porosity between dendrites, as well as segregations and carbides.

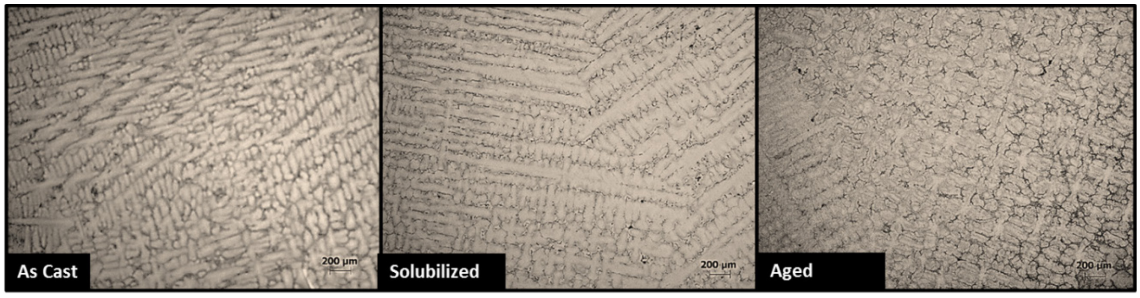


Figure 3. Images obtained by optical microscopy of the Inconel 713C material as cast, solubilized and aged condition.

In Fig. 3, it is possible to observe the elongation of the dendrites, as a consequence of the heat treatment of solubilization, causing an arrangement of the as cast structure towards a condition of greater thermodynamic equilibrium. This small microstructural change causes the stresses generated in the solidification to be better accommodated.

The microstructure with interdendritic precipitation of carbides (light phase) is highlighted in Fig. 4.

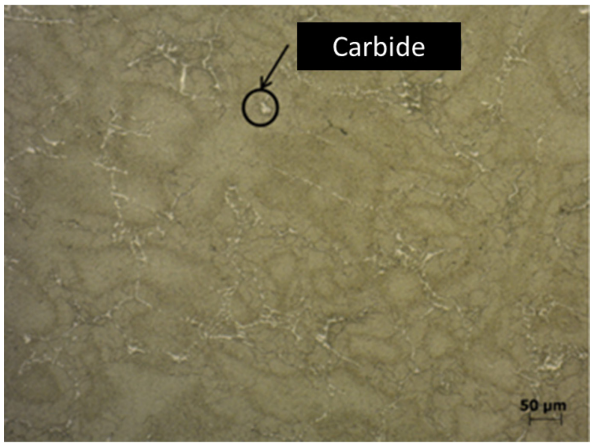


Figure 4. Carbides identified in the image obtained from optical microscopy in the aged condition.

Scanning electron microscopy (SEM) was performed on samples in the three heat treatment conditions. The samples were embedded and attacked, and the objective of the analysis was to observe microstructural differences occurring with the heat treatments. Micrographs were obtained using secondary electrons.

Fig. 5 shows the sample in the as cast condition, where it is possible to observe the matrix phase γ, the darkest region, and the γ' phase, the clearest region. The γ' phase is present in the intragranular form.

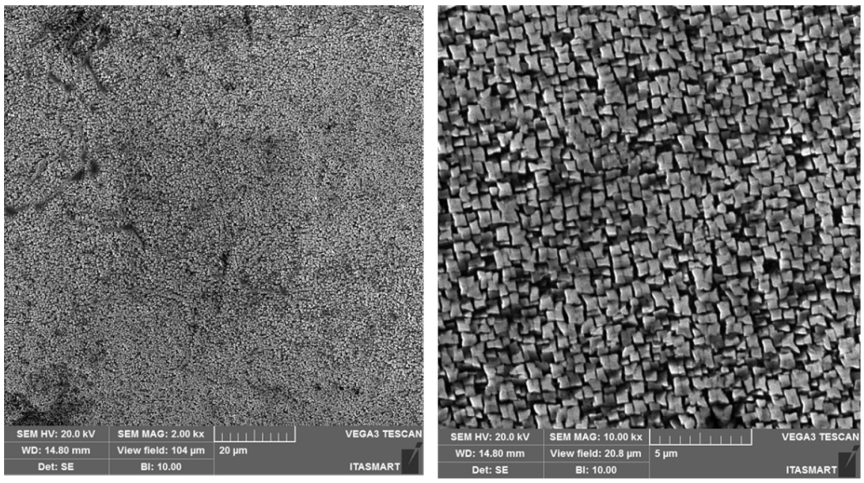


Figure 5. SEM of the as cast condition.

With the subsequent heat treatments, it was possible to show the higher distribution of the carbides along the matrix phase γ, as can be observed in Fig. 6. This distribution is related to the mobility of these atoms, leaving the concentrated veins of this element of the carbides and solubilizing still more in the matrix phase, both in the solubilized condition and mainly in the aged condition.

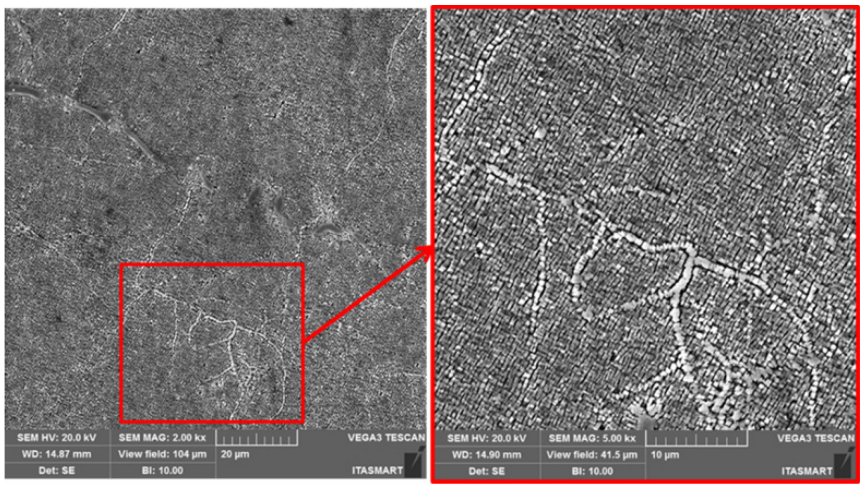


Figure 6. SEM of the aged condition.

***Energy-dispersive X-ray spectroscopy (EDS)***

Linear EDS analysis was performed to confirm the variation of the chemical elements in the microstructure, the results were described in Fig. 7. The analysis presents the variation of the chemical elements along a line passing through the fields of the matrix phase, along with the dispersed phase and the carbide veins.

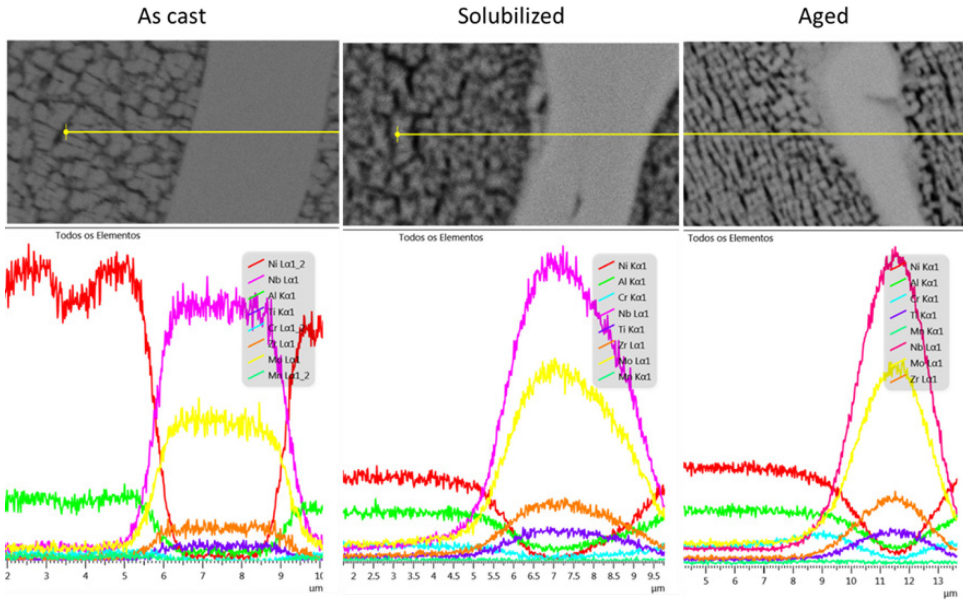


Figure 7. EDS of the samples in the three heat treatment conditions.

We show that in the γ and γ' phase there is a much higher presence of nickel than in the carbides, as well as aluminum, elements responsible for the formation of both phases. In the carbides, there is a considerable presence of niobium, molybdenum, zirconium, and titanium, these being the elements present in the carbides MC, $M_{23}C_6$, and $M_6C$.

With the heat treatments, we show a reduction in the niobium concentration in the carbides, which diffuses towards the γ matrix. With the treatment of aging, there is a higher concentration of niobium in the carbides, increasing well its concentration in relation to the others, molybdenum, zirconium, and titanium

***Thermocalculation of phase stability***

The simulation results of the percentage weight of each phase as a function of temperature are shown in Figs. 8 and 9. Figure 8 shows the major phases and the Fig. 9, the minority phases. The liquidus and solidus temperatures are 1,350 and 1,280°C, respectively, indicating a solidification range of 70°C. The first phase to solidify from the liquid is the matrix phase γ, the first carbides, MC-type, started to segregate around 1,360°C, with the ending of the liquid phase solidification,

both phases coexist at the end of solidification, forming a microstructure γ plus MC-type carbides in this range of temperature. The Ti, Nb, and Cr present in the alloy are carbide-forming elements.

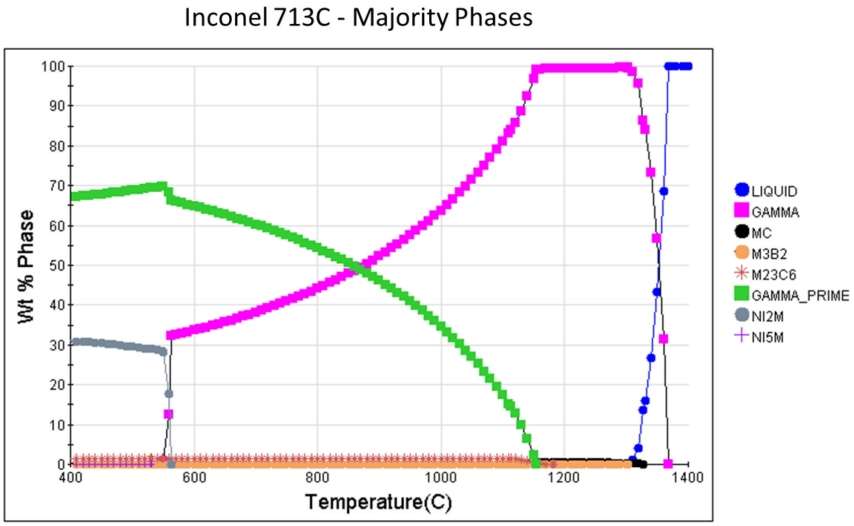


Figure 8. Percentage (in wt.%) of the majority phases vs temperature in Inconel 713C.

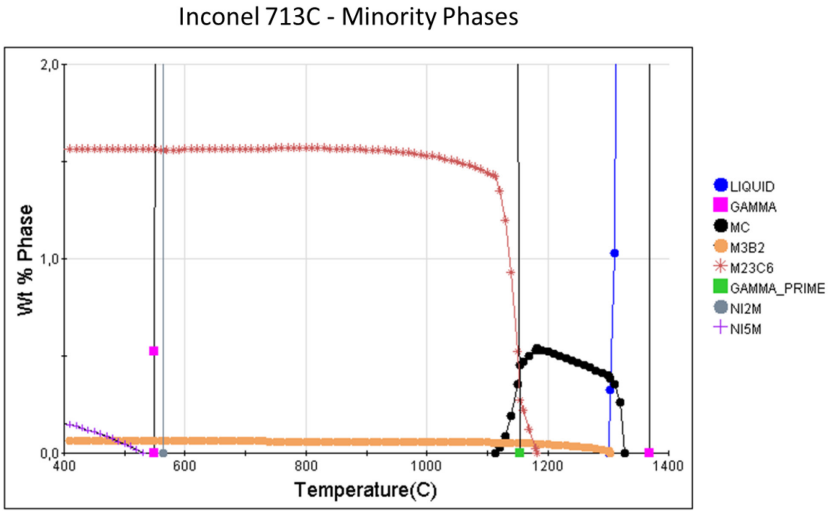


Figure 9. Percentage (in wt.%) of the minority phases vs temperature in Inconel 713C.

The predicted γ' solvus temperature is around 1,175°C where the phase starts increasing with the decrease in the γ phase percentage. In the minority phase graphic (Fig. 9), shows the stability of the carbides, the MC-type is stable from 1,360 to 1,160°C, at temperatures lower than 1,200°C the $M_{23}C_6$ is more stable, and a small percentage of boride $M_3B_2$-type is also stable.

## Conclusions

It can be concluded that the heat treatments of solubilization and aging of the Inconel 713C alloy alter the microstructure of the alloy with the formation of carbides and reduction of the acicularity of the dendritic structures. There is a change in the niobium concentration of the carbides, these hardening phases of the alloy. The final microstructure expected is matrix phase γ, solubilized γ' with a small percentage of carbide ($M_{23}C_6$-type) and boride ($M_3B_2$ type). The main objective of these heat treatments is the improvement of the mechanical properties of the alloy studied.

**Acknowledgments**

This research did not receive any specific grant from funding agencies in the public, commercial, or not-for-profit sectors.

**References**

[1] Aeromagazine. Novos aviões, motores e combustíveis. Disponível em: <http://aeromagazine.uol.com.br/artigo/novos-avioes-motores-e-combustiveis_890.html>. Acesso em: 30 nov. 2016.

[2] Backman, D.G.; Williams, J.C. Advanced materials for aircraft engine applications. Science, New Series: American Association for the Advancement of Science, vol. 255, n°. 5048, 1082-1087, 1992.

[3] Reis, A. G. ; Reis, D. A. P ; Moura Neto, C. ; Barboza, M. J. R. ; Onoro, J. . Creep behavior and surface characterization of a laser surface nitrided Ti-6Al-4V alloy. Materials Science & Engineering. A, Structural Materials: Properties, Microstructure and Processing, v. 577, 48-53, 2013.

[4] Sugahara, T.; Martinolli, K.; Reis, D.A.P.; Moura Neto, C.; Couto, A. A.; Neto, F. P.; Barboza, M.J.R. Creep Behavior of the Inconel 718 Superalloy. Defect and Diffusion Forum, v. 326-328, 509-514, 2012.

[5] Martinolli, K.; Sugahara, T.; Reis, D.A.P.; Moura Neto, C.; Hirschmann, A. C.; Couto, A. A. . Evaluation of Inconel 718 Creep Behavior. Defect and Diffusion Forum, v. 326-328, 525-529, 2012.

[6] Reis, D.A.P; Moura Neto, C.; Oliveira, A.C.C.; Couto, A.A. ; Domingues, N.I. ; Sepka, S. Effect of Artificial Aging on the Mechanical Properties of an Aerospace. Diffusion and Defect Data, Solid State Data. Part A, Defect and Diffusion Forum, v. 326, 193-198, 2012.

[7] Martinolli, K.; Moura Neto, C.; Oliveira, A.C.C.; REIS, D.A.P.; Couto, A.A.; Sugahara, T. Evaluation of Inconel 718 Creep Behavior. Diffusion and Defect Data, Solid State Data. Part A, Defect and Diffusion Forum, v. 326, 525-529, 2012.

[8] Reis, A. G.; Reis, D. A. P; Moura Neto, C.; Barboza, M.J.R.; Silva, C.R.M.; Piorino Neto, F.; Onoro, J. Influence of Laser Treatment on the Creep of the Ti-6Al-4V Alloy. Metallurgical and Materials Transactions. A, Physical Metallurgy and Materials Science, v. 42, 3031-3034, 2011.

[9] Reis, D.A.P; Moura Neto, C.; Silva, C.R.M. ; Barboza, M.J.R.; Piorino Neto, F. Effect of coating on the creep behavior of the Ti-6Al-4V alloy.. Materials Science & Engineering. A, Structural Materials: properties, microstructure and processing, v. 486, 421-426, 2008.

[10] Barboza, M.J.R.; Perez, E.A.C.; Medeiros, M.M.; Reis, D.A.P.; Nono, M.C.A.; Piorino, F.; Silva, C.R.M. Creep behavior of the Ti-6Al-4V and a comparison with titanium matrix composites.. Materials Science & Engineering. A, Structural Materials: properties, microstructure and processing, Inglaterra, v. 428, n.1-2, 319-326, 2006.

[11] Reis, D.A.P.; Silva, C.R.M.; Nono, M.C.A.; Barboza, M.J.R.; Piorino, F.; Perez, E.A.C. Effect of environment on the creep behavior of the Ti-6Al-4V alloy. Materials Science & Engineering. A, Structural Materials: properties, microstructure and processing, v. 399, 276-280, 2005.

[12]Kracke, A. Superalloys, the most successful alloy system of modern times – past, present and future. 7th International Symposium on Superalloy 718 and Derivatives. TMS (The Minerals, Metals & Materials Society), 2010.

[13] Muktinutalapati, N. R. A. Materials for gas turbines – an overview. Advances in gas turbine technology, 2011.

[14] Meyer, M.A.; Chawla, K. K. Princípios de metalurgia mecânica. São Paulo: Edgard Blüncher, cap. 14, p. 406-420, 1982.

[15] Azevedo, C. R. F.; Moreira, M.F.; Hippert, E. Nickel Superalloy (INCONEL 713C). Publicação IPT 2767, Instituto de Pesquisas Tecnológicas, São Paulo, 2001.

[16] Pratt and Whitney Aircraft. Engineering Properties of Alloy 713C. Material Engineering Section, 1965.

[17] SAE INTERNATIONAL. AMS 5391: Nickel Alloy, Corrosion and Heat-Resistant, Investment Castings 73Ni - 0.14C - 4.5Mo - 2.3Cb (Nb) - 0.75Ti - 6.0Al - 0.010B - 0.12Zr Vacuum Cast, As-Cast. Abr. 2014. 9 páginas.

[18] DATA BASE : Thermo-Calc Software TTNI8/Ni-based superalloys database version 8, http://www.thermocalc.com. Accessed 18 May 2018

[19] Farina, A. Metalografia das Ligas e Superligas de Níquel, Technical Report Villares Metals, Brasil, 2000.

[20] Kunz, L.; Lukáš, P.; Konečná, R. High-cycle fatigue of Ni-base superalloy 713C. International Journal of Fatigue. vol. 32, p. 908-913, 2010.

[21] Reed, R.C. The Superalloys: Fundamentals and Applications. Cambridge, Cambridge University Press, p. 33-114, 2006.

[22] Nalawade, S.A.; Sundararaman, M.; SINGH,J. B.; VERMA, A.; KISHORE, R. Precipitation of γ’ phase in δ-precipitated Alloy 718 during deformation at elevated temperatures. Materials Science and Engineering A, vol. 527, p.2906-2909, 2010.

[23] Valle, L. C. M. Efeitos da solubilização e do envelhecimento na microestrutura e nas propriedades mecânicas da superliga Inconel 718. 2010. 97p. Dissertação (Mestrado em Engenharia Metalúrgica e de Materiais) – Universidade Federal do Rio de Janeiro, Rio de Janeiro, p.13-22, 2010.

[24] Ezugwu, E. O.; Wang, Z. M.; Machado, A. R. The machinability of nickel-based alloys: a review. Journal of Materials Processing Technology, v.86, p. 1-16, 1999.

[25] Decker, R. F. The evolution of wrought age-hardenable superalloys - nickel: a century of innovation – overview, JOM, p. 32-36, 2006.